Title

Recent Trends in Stratospheric Chlorine From Very Short-Lived Substances

Journal

Journal of Geophysical Research: Atmospheres, 124(4)

ISSN

2169-897X

Authors

Hossaini, Ryan
Atlas, Elliot
Dhomse, Sandip S
et al.

Publication Date

2019-02-27

DOI

10.1029/2018jd029400

Peer reviewed

JGR Atmospheres

RESEARCH ARTICLE
10.1029/2018JD029400

Recent Trends in Stratospheric Chlorine From Very Short-Lived Substances

Ryan Hossaini[1], Elliot Atlas[2], Sandip S. Dhomse[3], Martyn P. Chipperfield[3], Peter F. Bernath[4,5], Anton M. Fernando[6], Jens Mühle[7], Amber A. Leeson[1], Stephen A. Montzka[8], Wuhu Feng[3,9], Jeremy J. Harrison[10,11], Paul Krummel[12], Martin K. Vollmer[13], Stefan Reimann[13], Simon O'Doherty[14], Dickon Young[14], Michela Maione[15], Jgor Arduini[15], and Chris R. Lunder[16]

[1]Lancaster Environment Centre, Lancaster University, Lancaster, UK, [2]Rosenstiel School of Marine and Atmospheric Science (RSMAS), University of Miami, Coral Gables, FL, USA, [3]School of Earth and Environment, University of Leeds, Leeds, UK, [4]Department of Chemistry and Biochemistry, Old Dominion University, Norfolk, VA, USA, [5]Department of Chemistry, University of Waterloo, Waterloo, ON, Canada, [6]Department of Physics, Old Dominion University, Norfolk, VA, USA, [7]Scripps Institution of Oceanography, University of California San Diego, La Jolla, CA, USA, [8]National Oceanic and Atmospheric Administration (NOAA), Boulder, CO, USA, [9]NCAS, University of Leeds, Leeds, UK, [10]Department of Physics and Astronomy, University of Leicester, Leicester, UK, [11]National Centre for Earth Observation, University of Leicester, Leicester, UK, [12]Climate Science Centre, CSIRO Oceans and Atmosphere, Aspendale, Victoria, Australia, [13]Laboratory for Air Pollution and Environmental Technology, Empa, Swiss Federal Laboratories for Materials Science and Technology, Duebendorf, Switzerland, [14]School of Chemistry, University of Bristol, Bristol, UK, [15]Department of Pure and Applied Sciences, University of Urbino, Urbino, Italy, [16]Norwegian Institute for Air Research, Kjeller, Norway

Key Points:
- Stratospheric chlorine from very short-lived substances increased by 3.8 ppt/year over 2004–2017, with a growth slowdown in 2015–2017
- Chlorine from short-lived substances improves model representation of upper stratospheric HCl trends
- Short-lived chlorine offsets the 2004–2017 rate of upper stratospheric HCl decline by 15%

Supporting Information:
- Supporting Information S1

Correspondence to:
R. Hossaini,
r.hossaini@lancaster.ac.uk

Citation:
Hossaini, R., Atlas, E., Dhomse, S. S., Chipperfield, M. P., Bernath, P. F., Fernando, A. M., et al. (2019). Recent trends in stratospheric chlorine from very short-lived substances. *Journal of Geophysical Research: Atmospheres*, *124*, 2318–2335. https://doi.org/10.1029/2018JD029400

Received 28 JUL 2018
Accepted 8 JAN 2019
Accepted article online 18 JAN 2019
Published online 16 FEB 2019

Abstract Very short-lived substances (VSLS), including dichloromethane (CH_2Cl_2), chloroform ($CHCl_3$), perchloroethylene (C_2Cl_4), and 1,2-dichloroethane ($C_2H_4Cl_2$), are a stratospheric chlorine source and therefore contribute to ozone depletion. We quantify stratospheric chlorine trends from these VSLS ($VSLCl_{tot}$) using a chemical transport model and atmospheric measurements, including novel high-altitude aircraft data from the NASA VIRGAS (2015) and POSIDON (2016) missions. We estimate $VSLCl_{tot}$ increased from 69 (±14) parts per trillion (ppt) Cl in 2000 to 111 (±22) ppt Cl in 2017, with >80% delivered to the stratosphere through source gas injection, and the remainder from product gases. The modeled evolution of chlorine source gas injection agrees well with historical aircraft data, which corroborate reported surface CH_2Cl_2 increases since the mid-2000s. The relative contribution of VSLS to total stratospheric chlorine increased from ~2% in 2000 to ~3.4% in 2017, reflecting both VSLS growth and decreases in long-lived halocarbons. We derive a mean $VSLCl_{tot}$ growth rate of 3.8 (±0.3) ppt Cl/year between 2004 and 2017, though year-to-year growth rates are variable and were small or negative in the period 2015–2017. Whether this is a transient effect, or longer-term stabilization, requires monitoring. In the upper stratosphere, the modeled rate of HCl decline (2004–2017) is −5.2% per decade with VSLS included, in good agreement to ACE satellite data (−4.8% per decade), and 15% slower than a model simulation without VSLS. Thus, VSLS have offset a portion of stratospheric chlorine reductions since the mid-2000s.

Plain Language Summary It is well established that long-lived halogen-containing compounds of anthropogenic origin, such as chlorofluorocarbons, have led to depletion of the stratospheric ozone layer. As production of these compounds is now controlled by the Montreal Protocol, the atmospheric abundance of chlorine/bromine is in decline, and the ozone layer should "recover" in coming decades. Here we consider the contribution of Very Short-Lived Substances to stratospheric chlorine. These compounds also have anthropogenic sources, though are much less efficient at destroying ozone compared to, for example, most chlorofluorocarbons (per molecule emitted) as they break down more readily close to Earth's surface. Using surface observations and atmospheric model simulations, we show that stratospheric chlorine from short-lived substances has increased since the early 2000s. This increase is also apparent from airborne measurements of their atmospheric abundance over the same period. Using the model in conjunction with satellite estimates of stratospheric chlorine, we show rising levels of short-lived substances may be causing upper stratospheric chlorine to decline at a slower rate relative to what would be expected in their absence. While this offset in the rate of chlorine decline is modest (15%), it is nonnegligible and should be considered in the analysis of stratospheric composition trends.

1. Introduction

The depletion of the global ozone layer by chlorine and bromine compounds is a well-established and persistent environmental issue (e.g., Solomon, 1999). It is predominately caused by chlorine and bromine radicals released from long-lived halocarbons, such as chlorofluorocarbons (CFCs) and halons, whose production is now controlled by the UN Montreal Protocol and its amendments (e.g., WMO, 2014). Owing to the Protocol's ongoing success, the atmospheric abundances of total chlorine and bromine are declining (e.g., Carpenter et al., 2014; Froidevaux et al., 2006; Montzka et al., 2003) and the ozone layer is projected to return to pre-1980s levels in the middle to latter half of this century in consequence (e.g., Chipperfield et al., 2017; Dhomse et al., 2018; Eyring et al., 2010; Solomon et al., 2016).

While the science underpinning ozone depletion is well understood, uncertainties in emissions of certain ozone-depleting compounds exist, which have the potential to influence future ozone projections. Notably, for example, long-term surface measurements show that emissions of CFC-11 have likely increased since 2012, despite its reported production being near zero (Montzka et al., 2018). Another example is the recent indication of increasing dichloromethane emissions since the early 2000s, based on a network of surface observations (Hossaini et al., 2015a; Hossaini et al., 2017) and measurements made in the upper troposphere (Leedham Elvidge et al., 2015; Oram et al., 2017). Dichloromethane (CH_2Cl_2), along with chloroform ($CHCl_3$), perchloroethylene (C_2Cl_4), and 1,2-dichloroethane ($C_2H_4Cl_2$), among others, are so-called Very Short-Lived Substances (VSLS)—compounds with mean surface lifetimes typically less than 6 months (e.g., Ko et al., 2003).

Over the past decade it has become clear that (a) natural brominated VSLS (e.g., $CHBr_3$) are a significant source of stratospheric bromine (e.g., Sala et al., 2014; Salawitch et al., 2005; Sturges et al., 2000; Wales et al., 2018), and (b) chlorinated VSLS (Cl-VSLS) are a small, but potentially increasing, source of stratospheric chlorine (Hossaini et al., 2015b). CH_2Cl_2 is the most abundant Cl-VSLS and its tropospheric abundance has increased approximately twofold since the early 2000s. In contrast, $CHCl_3$ has remained relatively stable since the mid-1990s, while C_2Cl_4 has been in long-term decline over the same period (Carpenter et al., 2014). The above Cl-VSLS are expected to have significant or predominately anthropogenic sources (Montzka et al., 2011). For example, CH_2Cl_2 is widely used as a solvent and in the production of foam agents, among other applications (Feng et al., 2018). A substantial portion of the estimated present-day global CH_2Cl_2 emission rate of ~1 Tg year (Hossaini et al., 2017) is expected to occur in Asia (Oram et al., 2017). While no long-term $C_2H_4Cl_2$ surface record exists, observed interhemispheric gradients suggest that it too has anthropogenic sources (Hossaini et al., 2016a).

Carpenter et al. (2014) estimated that Cl-VSLS contributed ~95 (50–145) parts per trillion (ppt) Cl to the stratospheric loading of inorganic chlorine in 2012. Hossaini et al. (2015b) used a global model to investigate the trend in stratospheric chlorine from Cl-VSLS between 2005 and 2013. They estimated a mean increase of 3.7 ppt Cl/year over this period, with the positive trend reflecting increasing CH_2Cl_2. Although the impact of this additional chlorine on stratospheric ozone is expected to have been modest over the last decade (Chipperfield et al., 2018), possible future increases in Cl-VSLS emissions could influence the time scale for stratospheric ozone recovery, particularly in polar regions (Hossaini et al., 2017). Such projections carry large uncertainties; however, they are important to consider to provide bounds on potential resulting ozone changes, especially given that large CH_2Cl_2 emission increases from major economies are projected under *business as usual* scenarios until 2030 (Feng et al., 2018). On the same basis, it is important that historical trends in stratospheric chlorine from VSLS are well quantified, so that possible future changes can be gauged from an accurate baseline.

The aim of this paper is to provide an up-to-date assessment of the stratospheric chlorine loading due to Cl-VSLS (CH_2Cl_2, $CHCl_3$, C_2Cl_4, $C_2H_4Cl_2$, and C_2HCl_3) and to examine trends over the 2000–2017 period. To achieve this, we use a 3-D chemical transport model (CTM) supported by a range of atmospheric observations. This includes novel high-altitude aircraft measurements of these compounds from campaigns in 2015 and 2016. Our analysis also focusses on (a) whether a signature of historical Cl-VSLS trends is present in long-term stratospheric HCl records, (b) quantifying the sensitivity of stratospheric chlorine from VSLS to uncertainties in VSLS chemistry and removal processes, and (c) estimating the contribution from other less prominent Cl-VSLS, based on available observational data. Section 2 describes the CTM and the model experiments that were performed. Section 3

describes the various observational data sets. Section 4 presents our results, and conclusions are given in section 5.

2. Model and Experiments

2.1. CTM

TOMCAT/SLIMCAT is an offline 3-D CTM (Chipperfield, 2006; Monks et al., 2017) that has been widely used for studies of chemistry and transport in the troposphere (e.g., McNorton et al., 2016; Richards et al., 2013) and stratosphere (e.g., Chipperfield, 2006; Dhomse et al., 2016, 2015). The CTM is forced by meteorological fields (winds, temperature, and humidity) taken from the European Centre for Medium-Range Weather Forecasts ERA-Interim reanalysis (Dee et al., 2011). Tracer advection is based on a conservation of second-order moments scheme (Prather, 1986) and convective transport is parameterized based on the mass flux scheme of Tiedtke (1989), as described by Feng et al. (2011). Turbulent boundary layer mixing follows the nonlocal scheme of Holtslag and Boville (1993). The configuration of the model used here employs a hybrid sigma-pressure (σ-p) vertical coordinate with 60 verticals levels extending from the surface to ~60 km. Simulations were performed at a horizontal resolution of 2.8° × 2.8°.

The tropospheric model configuration described above has been used extensively in VSLS-related studies (e.g., Hossaini et al., 2016b) and employs a simplified offline chemistry scheme, whereby monthly mean fields of the hydroxyl radical (OH) concentration are prescribed based on the climatology produced for the TransCom-CH_4 project (Patra et al., 2011). We assume a fixed tropospheric Cl atom concentration, $[Cl] = 1.3 \times 10^3$ atoms per cubic centimeter, based on the tropospheric mean [Cl] calculated by a recent global model study (Hossaini et al., 2016a). Note, this configuration of the model is here applied to calculate the stratospheric input of Cl-VSLS and their products and does not contain detailed stratospheric chemistry. A stratospheric model configuration, with a very detailed stratospheric chemistry scheme, is later used to investigate HCl trends (see section 4.5) with and without Cl-VSLS.

2.2. Source Gas Boundary Conditions and Chemistry

Four major Cl-VSLS were considered in our control ("BASE") simulation (CH_2Cl_2, $CHCl_3$, C_2Cl_4, and $C_2H_4Cl_2$). Constraint on the surface abundance of these source gases (SGs) was applied using a latitude-dependent boundary condition based on observed mole fractions (SG_{MF}), varying in five bands (60–90°N, 30–60°N, 0–30°N, 0–30°S, and 30–90°S). Although simple, this approach has been shown to reproduce upper tropospheric observations and trends of these compounds well (Hossaini et al., 2015b). For CH_2Cl_2 and C_2Cl_4, SG_{MF} is based on NOAA surface measurements and varies annually (e.g., Montzka et al., 2018). For $CHCl_3$, SG_{MF} is based on AGAGE measurements (e.g., Prinn et al., 2000) and also varies annually (Text S1 and Figure S1). For $C_2H_4Cl_2$ and C_2HCl_3 (a very minor compound), no long-term surface records are available, thus SG_{MF} is estimated based on observations from the 2009–2012 HIPPO mission (e.g., Wofsy et al., 2011, 2012), with no time trend in SG_{MF} applied. In addition to VSLS, long-lived carbon tetrachloride (CCl_4) and methyl chloroform (CH_3CCl_3) are included in the model. Like VSLS, these compounds are a source of phosgene, which constitutes a significant component of stratospheric chlorine (e.g., Fu et al., 2007). For CCl_4 and CH_3CCl_3, a global SG_{MF} was prescribed.

For each VSLS, the BASE run considered chemical loss through OH oxidation, Cl atom oxidation, and photolysis, with the relevant kinetic parameters (rate constants, absorption cross sections, see Tables S1 and S2) mostly taken from the Jet Propulsion Laboratory data evaluation (Burkholder et al., 2015). Sensitivity experiments were performed to assess the significance of tropospheric VSLS oxidation by Cl (see section 2.4).

2.3. Product Gases

The oxidation of chlorine-containing VSLS has been considered in past WMO/UNEP Ozone Assessments (e.g., Ko et al., 2003) and in recent modeling work (Hossaini et al., 2016a). Here we adopted a simplified treatment of product gas (PG) chemistry, considering two idealized PG tracers, phosgene ($COCl_2$) and inorganic chlorine (Cl_y), thus allowing many long integrations of the model to be performed.

2.3.1. Phosgene

$COCl_2$ is an expected major product of $CHCl_3$ and C_2Cl_4 oxidation (Ko et al., 2003), as demonstrated by experimental and theoretical studies (e.g., Christiansen & Francisco, 2010a, 2010b; Tuazon et al., 1988). The $COCl_2$ yield from reaction of $CHCl_3$, C_2Cl_4, and C_2HCl_3 with OH has been reported to be 1.0, 0.47, and 0.4, respectively (Kindler et al., 1995). For these compounds, $COCl_2$ production in the model is calculated based on the above experimentally determined yields.

Little is currently known regarding the yield of $COCl_2$ from CH_2Cl_2 oxidation, with limited information in the literature. Although some experimental evidence for $COCl_2$ production from CH_2Cl_2 oxidation is available (Catoire et al., 1996; Sanhueza & Heicklen, 1975; Spence et al., 1976), $COCl_2$ was not noted as a major product of CH_2Cl_2 by Ko et al. (2003). In this work, we calculate $COCl_2$ production from CH_2Cl_2 "online" in the model based on the principal steps involved in the oxidation chain, as outlined below.

The initial oxidation of CH_2Cl_2 by either OH or Cl atoms ((R1), (R2)) produces a chlorinated peroxy radical ($CHCl_2O_2$):

$$CH_2Cl_2 + OH\ (+O_2) \rightarrow CHCl_2O_2 + H_2O \quad \text{(R1)}$$

$$CH_2Cl_2 + Cl\ (+O_2) \rightarrow CHCl_2O_2 + HCl \quad \text{(R2)}$$

The peroxy radical can undergo one of several different reactions. Under high NO_x conditions, such as in urban areas, reaction with NO (or NO_3) will likely dominate loss of $CHCl_2O_2$, leading to production of the alkoxy radical, $CHCl_2O$.

$$CHCl_2O_2 + NO \rightarrow CHCl_2O + NO_2 \quad \text{(R3)}$$

$$CHCl_2O_2 + NO_3 \rightarrow CHCl_2O + NO_2 + O_2 \quad \text{(R4)}$$

(R3) and (R4) are not phosgene forming channels as $CHCl_2O$ is expected to decompose to CHClO + Cl (e.g., Catoire et al., 1996). The atmospheric fate of CHClO is poorly known but sinks are expected to include atmospheric removal via heterogeneous and multiphase deposition processes (e.g., Ko et al., 2003; Toyota et al., 2004).

Alternatively, CH_2ClO_2 may react with HO_2 or RO_2 (e.g., Catoire et al., 1996), especially in low NO_x regions, through several phosgene-forming channels (R5, R6).

$$CHCl_2O_2 + HO_2 \rightarrow CHCl_2OOH + O_2, \quad \text{(R5a)}$$

$$\rightarrow COCl_2 + H_2O + O_2 \quad \text{(R5b)}$$

$$\rightarrow CHClO + HOCl + O_2 \quad \text{(R5c)}$$

$$CHCl_2O_2 + CH_3O_2 \rightarrow CHCl_2O + \text{products}, \quad \text{(R6a)}$$

$$\rightarrow CHCl_2OH + \text{products} \quad \text{(R6b)}$$

$$\rightarrow COCl_2 + \text{products} \quad \text{(R6c)}$$

Branching ratios for reactions with HO_2 were taken from the most recent IUPAC evaluation (Atkinson et al., 2008), while for RO_2 they are from the Master Chemical Mechanism version 3.3.1 (http://mcm.leeds.ac.uk/MCM/). For R5a–R5c the branching ratios are 0, 0.7 and 0.3, respectively, while for R6a–R6c they are 0.6, 0.2 and 0.2. Note, in addition to (R5b) and (R6c), $COCl_2$ is also expected to be produced from (R6b), owing to the subsequent degradation of the $CHCl_2OH$ alcohol (Master Chemical Mechanism, v3.3.1).

Based on the above, the $COCl_2$ yield (Y) from CH_2Cl_2 oxidation is computed in all model grid boxes on every time step according to equation (1), where k_3, k_4, k_5, and k_6 are rate constants for the reactions of $CHCl_2O_2$ with NO, NO_3, HO_2, and CH_3O_2, respectively.

$$Y = (0.7k_5[HO_2] + 0.4k_6[CH_3O_2])/(k_3[NO] + k_4[NO_3] + k_5[HO_2] + k_6[CH_3O_2]). \quad (1)$$

An expression for $COCl_2$ production from CH_2Cl_2 is thus: CH_2Cl_2 + OH → Y $COCl_2$ + (2-2Y) Cl_y. Typical Y values strongly dependent on the local NO_x concentration and are found to be in the range of ~0.05 to 0.1

Table 1
Summary and Brief Description of TOMCAT/SLIMCAT Model Experiments

Model run	Description
BASE	Control run: see main text
EXP1	As BASE but CH_2Cl_2 and C_2Cl_4 surface boundary conditions from AGAGE
EXP2	As BASE but no Cl sink of source gases
EXP3	As BASE but upper limit of PGI (no tropospheric Cl_y and $COCl_2$ removal)
EXP4	As BASE but repeating meteorology
EXP5	As BASE but 25% increase in tropospheric [OH]
EXP6	As BASE but 25% decrease in tropospheric [OH]
EXP7	As BASE but fixed phosgene yield (Y) from CH_2Cl_2 of 1
EXP8	As EXP3 but fixed phosgene yield (Y) from CH_2Cl_2 of 1

Note. PGI = Product Gas Injection.

over industrialized regions and >0.3 over the oceans (see discussion in Text S2). Separate $COCl_2$ tracers were included in the model, allowing its production from individual SGs to be tagged. In addition to production from VSLS, the model also considers $COCl_2$ derived from long-lived CCl_4 and CH_3CCl_3, the former of which is the main stratospheric phosgene source (Kindler et al., 1995).

$$CCl_4 + h\nu \rightarrow COCl_2 + 2Cl \quad (R7)$$

$$CH_3CCl_3 + OH \rightarrow COCl_2 + Cl \quad (R8)$$

Removal of $COCl_2$ in the model occurs through photolysis (R9) and by washout. The latter is approximated in the model troposphere using a prescribed washout lifetime of 58 days (Kindler et al., 1995; Ko et al., 2003). The sensitivity of our results to this assumption and to uncertainties in the $COCl_2$ yield calculation were examined (see also section 2.4).

$$COCl_2 + h\nu \rightarrow 2Cl + CO \quad (R9)$$

2.3.2. Inorganic Chlorine (Cl_y)

All non-$COCl_2$ PGs arising from $CHCl_3$, CH_2Cl_2, C_2Cl_4, $C_2H_4Cl_2$, and C_2HCl_3 oxidation were grouped in five generic Cl_y tracers, without further partitioning. These five Cl_y tracers were tagged allowing their production to be tracked to parent SGs. In the troposphere, Cl_y is dominated by highly soluble HCl (e.g., Hossaini et al., 2016a). The washout lifetime of Cl_y in the model was set to 5 days, based on the reported Cl_y lifetime from a recent detailed GEOS-Chem 3-D model study (Sherwen et al., 2016). The sensitivity of our findings to this lifetime were examined.

2.4. Base Simulation and Sensitivity Experiments

Our BASE (control) simulation, described in the previous sections, was spun-up for a period of 5 years and then run over an 18-year analysis period (2000 to 2017). Additionally, a series of model sensitivity runs were performed in which various parameters and processes were adjusted one-by-one with respect to the BASE run (Table 1). In EXP1, the CH_2Cl_2 and C_2Cl_4 surface boundary conditions were prescribed according to AGAGE data (compared to NOAA in the BASE run). In EXP2, the Cl atom sink of VSLS was switched off. In EXP3, tropospheric wet removal of $COCl_2$ and Cl_y was switched off to give an upper limit to their potential contribution to stratospheric chlorine. In EXP4, repeating year 2000 meteorology was used throughout the simulation so that the influence of varying dynamics on the stratospheric input of VSLS could be assessed (i.e., comparing BASE to EXP4).

In EXP5 and EXP6, tropospheric [OH] was increased or decreased by 25%, respectively. This OH perturbation was chosen as it is approximately equal to the spread in tropospheric [OH] from the models that took part in the ACCMIP intercomparison (Voulgarakis et al., 2013). The $COCl_2$ yield from CH_2Cl_2 (i.e., Y in equation (1)) was fixed to 1 globally in EXP7 and EXP8, which were otherwise identical to the BASE run or EXP3, respectively. The results from these sensitivity runs are discussed in section 4.4, in the context of their influence on total chlorine from VSLS delivered to the stratosphere.

3. Observations

3.1. High-Altitude Aircraft Measurements

Cl-VSLS observations from eight NASA aircraft missions between 2004 and 2016 were considered in this work (Table 2). As the measurements were obtained by the same group (the University of Miami), the possible influence of different calibration scales (used by different laboratories) on reported mole fractions is minimized. Each of the aircraft campaigns measured the principal Cl-VSLS, CH_2Cl_2, $CHCl_3$, C_2Cl_4, and $C_2H_4Cl_2$. Such observations are particularly valuable in the case of $C_2H_4Cl_2$, due to the absence of long-term surface measurements, but have yet to be examined in detail. In addition to the above compounds, measurements of other relatively minor Cl-VSLS are available from some of the campaigns. These include chlorobenzene (C_6H_5Cl), chloroethane (C_2H_5Cl), and trichloroethylene (C_2HCl_3). Similarly, in the

Table 2
Summary of Aircraft Campaign Data Used in This Study

Mission	Mon/year	Area	Species measured	Ref
Pre-AVE	January–February 2004	Central America	$CH_2Cl_2/CHCl_3/C_2Cl_4/C_2H_4Cl_2/C_2HCl_3$	a, e
CR-AVE	January–February 2006	Central America	$CH_2Cl_2/CHCl_3/C_2Cl_4/C_2H_4Cl_2/C_2H_5Cl$	a, f
TC4	August 2007	Central America	$CH_2Cl_2/CHCl_3/C_2Cl_4/C_2H_4Cl_2/C_2HCl_3$	b, g
ATTREX	November 2011	E. Pacific	$CH_2Cl_2/CHCl_3/C_2Cl_4/C_2H_4Cl_2$	c, d, h
ATTREX	February–March 2013	E. Pacific	$CH_2Cl_2/CHCl_3/C_2Cl_4/C_2H_4Cl_2/C_6H_5Cl$	
ATTREX	January–March 2014	W. Pacific	$CH_2Cl_2/CHCl_3/C_2Cl_4/C_2H_4Cl_2/C_2HCl_3/C_6H_5Cl$	
VIRGAS	October 2015	Gulf of Mexico	$CH_2Cl_2/CHCl_3/C_2Cl_4/C_2H_4Cl_2/C_6H_5Cl$	i
POSIDON	October 2016	W. Pacific	$CH_2Cl_2/CHCl_3/C_2Cl_4/C_2H_4Cl_2/C_2HCl_3/C_6H_5Cl$	j

[a]Hagan et al. (2004), Park et al. (2007). [b]Pfister et al. (2010). [c]Jensen et al. (2017). [d]Navarro et al. (2015). [e]https://espoarchive.nasa.gov/archive/browse/pre_ave [f]https://espo.nasa.gov/ave-costarica2/ [g]https://espo.nasa.gov/tc4/ [h]https://espo.nasa.gov/attrex/content/ATTREX [i]https://www-air.larc.nasa.gov/missions/virgas/ [j]https://espo.nasa.gov/posidon/

absence of long-term surface measurements, the aircraft data provide useful constraint on their tropospheric abundance.

The location of the measurement campaigns is indicated in Figure S2. The campaigns sampled around Central America (Pre-AVE 2004, CR-AVE 2006, TC4 2007, ATTREX 2011, VIRGAS 2015), the East Pacific (ATTREX 2013), and the West Pacific (ATTREX 2014, POSIDON 2016). Measurements of Cl-VSLS from the two most recent campaigns (VIRGAS and POSIDON) have yet to be reported in the literature. The VIRGAS (Volcano-plume Investigation Readiness and Gas-phase & Aerosol Sulfur) mission was conducted around the Gulf of Mexico in October 2015 (https://www.esrl.noaa.gov/csd/projects/virgas/). Measurements of Cl-VSLS were obtained from whole air samples collected on board six flights of the NASA WB-57 high-altitude research aircraft. The POSIDON (Pacific Oxidants, Sulfur, Ice, Dehydration, & Convection) mission was centered around Guam in the tropical West Pacific (https://espo.nasa.gov/posidon/). Cl-VSLS measurements were also obtained from whole air samples during 10 WB-57 flights in October.

3.2. Satellite Measurements of $COCl_2$ and HCl

We consider atmospheric measurements of $COCl_2$ from the Atmospheric Chemistry Experiment Fourier Transform Spectrometer (ACE-FTS), onboard the SCISAT satellite (Bernath, 2017). The ACE $COCl_2$ data have been previously described in Fu et al. (2007) and Brown et al. (2011), and briefly considered by Hossaini et al. (2015b). Here we use version 3.5/3.6 ACE $COCl_2$ data in 2014 and 2015 to assess the fidelity of the model $COCl_2$ simulation in the tropical upper troposphere/lower stratosphere. For HCl, we consider the ACE measurement data set described by Bernath and Fernando (2018). Briefly, ACE HCl volume mixing ratios (version 3.5/3.6) were filtered at each pressure level by removing all values that were outside 2.5 standard deviations from the median. Quarterly averages were obtained for December–February, March–May, June–August, and September–November at each pressure level, making a HCl time series covering March–May 2004 to September–November 2017. The time series at each pressure level was deseasonalized and linear trends were calculated as described by Bernath and Fernando (2018). These trends are considered in section 4.5, with corresponding model trends calculated in the same fashion.

The standard error on the ACE and model HCl trend estimates was calculated using the method of Weatherhead et al. (1998), following Bernath and Fernando (2018), which includes a term considering the effect of first-order autocorrelation in the time series of residuals. In section 4.5, trend errors are presented with ±2 standard error uncertainty.

4. Results and Discussion

4.1. SGs Lifetimes

We first consider the tropospheric lifetimes of CH_2Cl_2, $CHCl_3$, C_2Cl_4, and $C_2H_4Cl_2$. The total local lifetime (τ_{tot}) of each SG is shown in Figure 1 (expressed as an annual and zonal mean). The total local lifetime of VSLS (e.g., Ko et al., 2003) is defined from the partial SG lifetimes with respect to oxidation via OH (τ_{OH})

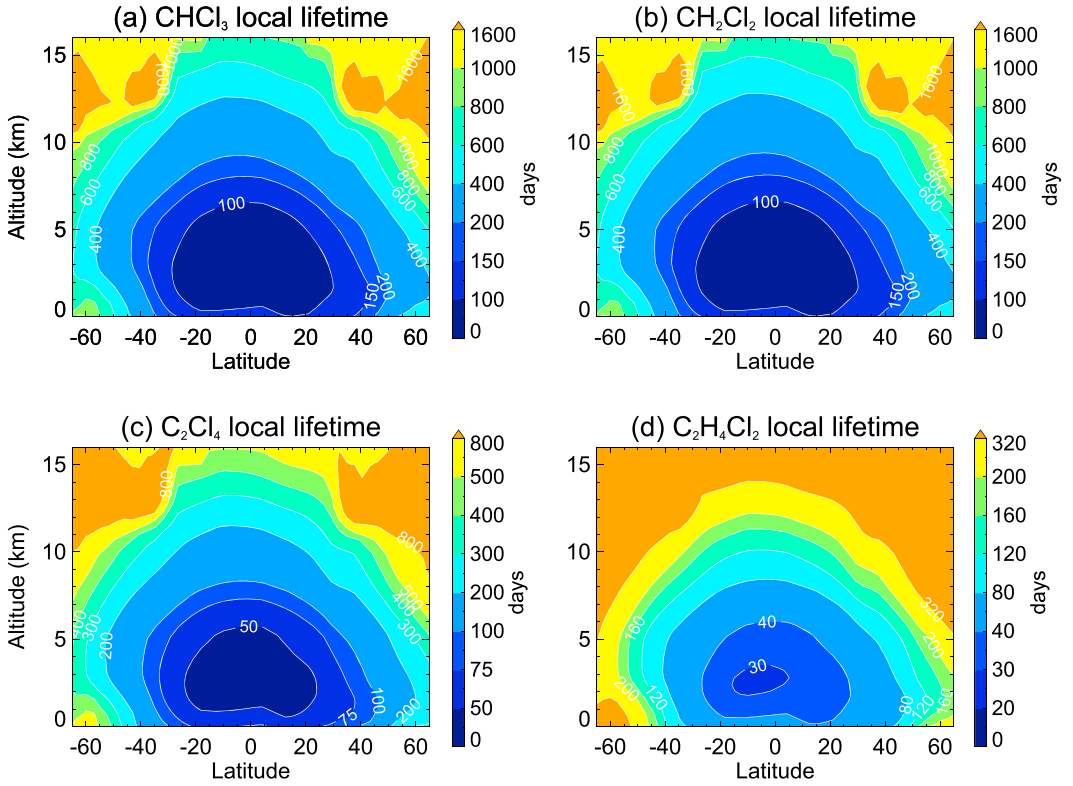

Figure 1. Local lifetime (days) of (a) $CHCl_3$, (b) CH_2Cl_2, (c) C_2Cl_4 and (d) $C_2H_4Cl_2$. The annual zonal mean local lifetime (τ_{tot}) is calculated from partial lifetimes with respect to OH oxidation and photolysis (see section 4.1). Note the differing scales between panels.

and photolysis ($\tau_{h\nu}$); that is, $\tau_{tot}^{-1} = (\tau_{OH})^{-1} + (\tau_{h\nu})^{-1}$. The lifetime data presented in Figure 1 are based on EXP2; that is, the model run that considers these sinks but not oxidation of SGs via Cl atoms.

As with all VSLS, local lifetimes vary substantially with location (and season). For $CHCl_3$ and CH_2Cl_2, the two SGs with the longest lifetimes, annual mean τ_{tot} for the tropical boundary layer is ~102 days (Table 3). Similarly, τ_{tot} is ~61 and ~43 days for C_2Cl_4 and $C_2H_4Cl_2$, respectively. These calculated lifetimes are within ~10% of those reported by Carpenter et al. (2014). As has been reported for brominated VSLS, notably CH_2Br_2 (Hossaini et al., 2010), the local lifetime of chlorinated VSLS varies substantially with altitude. For example, in the cold tropical upper troposphere (~10 km), where temperature-dependent loss rates via OH are relatively slow, τ_{tot} is a factor of around two to three times larger for each compound, compared to at the surface.

For $CHCl_3$, CH_2Cl_2, and $C_2H_4Cl_2$, Cl atoms are found to be a negligible tropospheric sink. As photolysis is also a negligible tropospheric sink (Carpenter et al., 2014), τ_{tot} effectively equals τ_{OH} for these species. However, for C_2Cl_4 we find that its local lifetime is strongly affected by inclusion of the tropospheric Cl sink

Table 3
Annual Mean Local Lifetime of Cl-VSLS (Days) With Respect to OH Oxidation and Comparison to WMO (2014)

	Boundary layer		Upper troposphere (~10 km)	
Species	This work	WMO (2014)	This work	WMO (2014)
$CHCl_3$	102 (93–114)	112 (100–136)	252 (245–258)	190 (182–197)
CH_2Cl_2	102 (93–114)	109 (98–133)	245 (238–250)	179 (171–185)
C_2Cl_4	61[a] (55–68)	67 (60–81)	158[b] (154–162)	119 (114–123)
$C_2H_4Cl_2$	43 (39–48)	47 (42–58)	127 (124–130)	(86–93)

Note. The values in parentheses indicate seasonal range.
[a]49 (45–53) days when C_2Cl_4 + Cl reaction included. [b]86 (84–87) days when C_2Cl_4 + Cl reaction included.

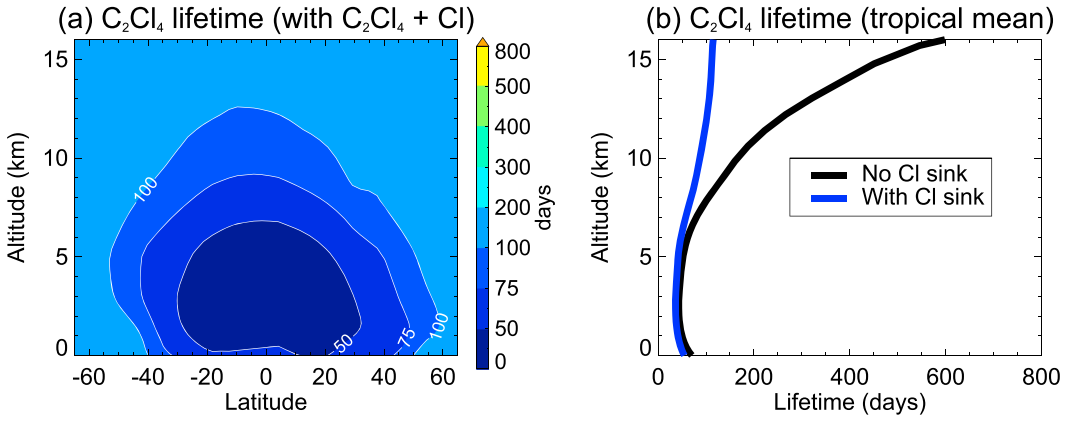

Figure 2. (a) C_2Cl_4 local lifetime (days) when the C_2Cl_4 + Cl sink is considered (in addition to loss via OH and photolysis). For comparison, the contour levels and scale are the same as those in panel (d) of Figure 1. (b) Tropical mean profile of C_2Cl_4 local lifetime calculated with (blue) and without (black) the C_2Cl_4 + Cl sink.

(i.e., comparing EXP2 with the BASE run). For example, τ_{tot} varies from ~49 days in the tropical boundary layer to ~86 days at 10 km, when C_2Cl_4 + Cl is included (BASE simulation). Excluding the Cl sink (i.e., EXP2) increases these values to ~61 and ~158 days, respectively; that is, τ_{tot} is up to a factor ~2 larger (Table 3). Recall that EXP2 assumes a background tropospheric [Cl] of 1.3×10^3 atoms per cubic centimeter, based on a recent global model estimate (Hossaini et al., 2016a). In section 4.2 we consider whether inclusion of the Cl atom sink improves model/measurement agreement of C_2Cl_4 in the upper troposphere, where its impact is greatest (Figure 2).

While the concept of a single, globally applicable, lifetime (defined by global burden/global removal rate) is generally not appropriate for VSLS, such values are used by box models to infer surface emissions (e.g., WMO, 2014). On this basis and for completeness, we report the following mean lifetimes from this study: 168 (CH_2Cl_2), 174 ($CHCl_3$), 101 (C_2Cl_4, no Cl sink), 68 (C_2Cl_4, with Cl sink), and 77 days ($C_2H_4Cl_2$).

4.2. SG Injection

We differentiate between chlorine input to the stratosphere from (a) chlorine atoms in the form of emitted SGs (SG Injection, SGI) and (b) from organic/inorganic PGs released from SG degradation in the troposphere (PG Injection, PGI). The annual tropical mean stratospheric chlorine input due to SGI is shown in Figure 3. Results are shown primarily from the BASE run (solid lines), though output from EXP2 (no Cl sink of VSLS) is also shown for C_2Cl_4 (dashed line, Figure 3c). Figure 3 also shows measurement-based estimates of chlorine SGI (filled circles) derived from various high-altitude aircraft observations (section 3.1). The open symbols show the model sampled at the measurement locations/times for the four most recent campaigns (although our model SGI estimates are reported as tropical annual means).

From the BASE run, we estimate that total chlorine SGI (Figure 3f) increased from ~55 (±10) ppt Cl in 2000 to ~93 (±17) ppt Cl in 2017. Of the present-day total, CH_2Cl_2 is the largest contributor (~70%), followed by $CHCl_3$ (~18%), $C_2H_4Cl_2$ (~9%), and C_2Cl_4 (~2%). The observation data provide some constraint on the contribution from known potential "other" Cl-VSLS that were not included in our model: for example, C_6H_5Cl and C_2H_5Cl. Although the data are limited, it suggests that the sum of chlorine in these three minor species is <1 ppt Cl around the tropopause and that they thus make a negligible contribution to chlorine SGI. Our total SGI estimate (Table 4) is at the upper limit of the 72 (50–95) ppt Cl SGI range reported in the 2014 Ozone Assessment (Carpenter et al., 2014) that was appropriate for the year 2012. This reflects that we consider the most recent VSLS trends, including increases in CH_2Cl_2 since that assessment. For comparison, our corresponding 2012 modeled SGI estimate is 76 (±13) ppt Cl, in reasonable agreement to Carpenter et al. (2014).

From Figure 3, the model generally captures the measured total chlorine SGI well, which was observed to be similar during the 2013 ATTREX (102 ± 13 ppt Cl), 2014 ATTREX (105 ± 11 ppt Cl), and 2015 VIRGAS (104 ± 15 ppt Cl) missions. For example, when sampled at the measurement locations, the equivalent model estimate for the VIRGAS campaign is ~110 ppt Cl. The observed SGI from the most recent campaign,

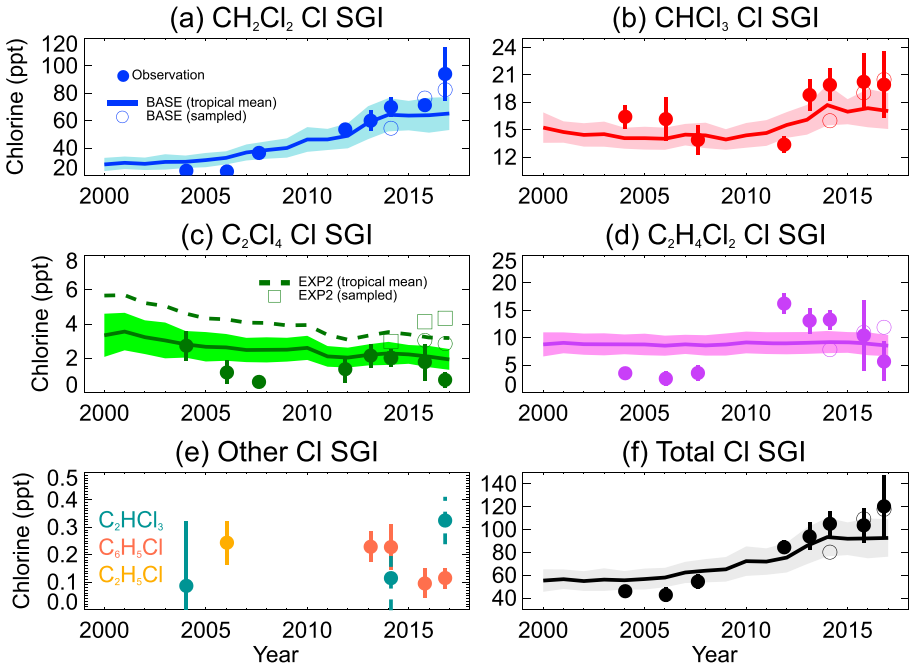

Figure 3. Stratospheric source gas chlorine injection (ppt Cl) from (a) CH_2Cl_2, (b) $CHCl_3$, (c) C_2Cl_4, (d) $C_2H_4Cl_2$, (e) other very short-lived substances, and (f) total SGI. Model results (solid lines, shading denotes ±1σ) are from experiment BASE (tropical annual means) forced by surface data (section 2.2). Observed quantities (filled circles) are averages (vertical bars denote ±1 standard deviation) for available aircraft data between 16.5–17.5 km in the tropics (±20° latitude) from the following campaigns: 2004 (Pre-AVE), 2006 (CR-AVE), 2007 (TC4), 2011 (ATTREX), 2013 (ATTREX), 2014 (ATTREX), 2015 (VIRGAS), and 2016 (POSIDON). The location of these campaigns is summarized in Figure S2. The open symbols represent BASE output sampled at the measurement location/times. For C_2Cl_4 (panel c), model output from EXP2 (dashed line) is also shown; that is, not including the C_2Cl_4 + Cl sink. Note, "other very short-lived substances" (C_2HCl_3, C_6H_5Cl, and C_2H_5Cl) that are observed but not modeled are not counted in total SGI (panel f) as their contribution seems insignificant. SGI = source gas injection.

POSIDON in 2016, was ~120 (±27) ppt Cl, also in good agreement to our campaign-sampled model (118 ± 6 ppt Cl). In principle, the relatively large chlorine SGI from the POSIDON mission, conducted in the West Pacific, could have been influenced by proximity to major VSLS source regions (e.g., Oram et al., 2017). However, we note that the campaign-sampled model output—with no zonal variability in VSLS loading at the surface—agrees well with the measurement data. The implication of this is that spatiotemporal variability in (a) Cl-VSLS troposphere-to-stratosphere transport and/or (b) Cl-VSLS tropospheric lifetimes is a significant influence on regional SGI variability. This is also reflected in the difference between the model tropical average SGI (sold lines, Figure 3) versus the open circles (campaign-sampled).

Table 4
Modeled Stratospheric Chlorine Input (ppt Cl) Due to Source Gas Injection, Product Gas Injection and Total

	Contribution to stratospheric chlorine (ppt Cl)			
Species	SGI	PGI ($COCl_2$)	PGI (Cl_y)	SGI + PGI
CH_2Cl_2	65.2 (±12.0)	2.0 (±0.2)	8.3 (±3.0)	75.5 (±15.2)
$CHCl_3$	17.1 (±2.0)	2.5 (±0.4)	1.0 (±0.4)	20.6 (±2.8)
C_2Cl_4	1.9 (±0.6)	0.5 (±0.1)	1.2 (±0.4)	3.6 (±1.1)
$C_2H_4Cl_2$	8.5 (±1.9)	-	2.2 (±0.7)	10.7 (±2.6)
C_2HCl_3	<0.01	0.22 (±0.04)	0.26 (±0.05)	0.48 (0.09)
Total Cl	~93 (±17)	5 (±0.7)	13 (±4.6)	111 (±22)

Note. Average 2017 values (±1 standard deviation) are calculated from the BASE simulation. SGI = source gas injection; PGI = product gas injection.

For individual SGs, the modeled SGI time series reflects known surface trends, including increases in CH_2Cl_2 since the mid-2000s, relatively stable levels of $CHCl_3$ until ~2010 following a small increase, and long-term decreases in C_2Cl_4 (Figure S1). Despite our relatively simple approach to constraining these Cl-VSLS at the surface, model-measurement agreement is reasonable throughout the simulation period, particularly for CH_2Cl_2 and $CHCl_3$, the most abundant compounds (see also Figures S3–S5). While aircraft measurements are somewhat sporadic and therefore should not be used in isolation as an indicator of robust long-term trends, the observations in Figure 3 show the signature of increasing CH_2Cl_2 between 2004 and 2016. This corroborates the reported CH_2Cl_2 increases from surface records (e.g., Hossaini et al., 2017) and measurements in the upper troposphere (Leedham Elvidge et al., 2015).

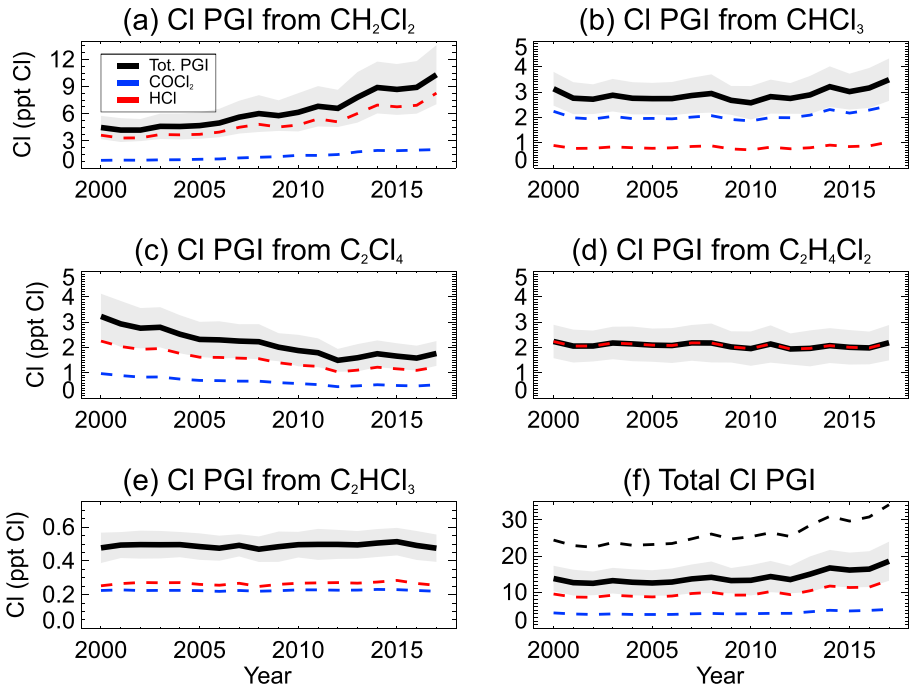

Figure 4. Modeled annual mean stratospheric chlorine product gas injection (ppt Cl) originating from (a) CH_2Cl_2, (b) $CHCl_3$, (c) C_2Cl_4, (d) $C_2H_4Cl_2$, (e) C_2HCl_3, and (f) total PGI. Dashed lines denote the PGI contribution from the idealized $COCl_2$ (blue) and Cl_y (red) tracers. The solid lines denote the total PGI (i.e., the sum of $COCl_2$ and Cl_y contributions), with shading denoting ±1 standard deviation from the mean. Model output is from experiment BASE, though in panel (f) the total PGI from EXP3 (upper limit for PGI) is also shown (dashed black line). PGI = product gas injection.

The "leveling off" of the model CH_2Cl_2 SGI time series in Figure 3a is driven by the model surface boundary conditions, based on surface observations, which in turn reveal an apparent slowdown in tropospheric CH_2Cl_2 growth. This is further discussed in section 4.5 in the context of total chlorine from VSLS. Note, in the case of $C_2H_4Cl_2$, for which no time trend in the model was applied, the observed data do not appear to show a clear trend and suggest an SGI contribution of the order of ~5–15 ppt Cl in 2014–2016.

Switching off the Cl atom sink of individual VSLS made a negligible difference to the calculated chlorine SGI in our model, apart for C_2Cl_4. Modeled SGI from C_2Cl_4 is ~65% larger in EXP2 (without the C_2Cl_4 + Cl sink) relative to the BASE simulation, and this leads to significantly poorer agreement to the aircraft data. On this basis, the +Cl reaction should be included in models and the resulting lower lifetime (section 4.1) considered in relevant box-model emission calculations.

4.3. PGI

Figure 4 shows the modeled stratospheric chlorine PGI due to $COCl_2$ and Cl_y from individual SGs (Figures 4a–4e), along with the total chlorine PGI from VSLS (Figure 4f). Degradation products from CH_2Cl_2 are the largest contributors to the overall PGI, accounting for ~57% of the total (Table 4). From the BASE simulation, we estimate chlorine PGI from CH_2Cl_2 increased from ~4.5 (±1.3) ppt Cl in 2000 to ~10.3 (±3.2) ppt Cl in 2017. Over the same period PGI due to C_2Cl_4 decreased by ~1.5 ppt Cl in response to its declining tropospheric abundance, offsetting some of this increase from CH_2Cl_2. In contrast, PGI due to $CHCl_3$ products remained relatively stable over the simulation period (~3.5 ± 0.8 ppt Cl in 2017). Our best estimate of total chlorine PGI (BASE run) is ~13.8 (±3.5) ppt Cl in 2000, rising to ~18.6 (±5.2) ppt Cl in 2017. Of the present-day PGI total, ~13 ppt Cl is in inorganic form (Cl_y), in agreement with the 10 (0–20) ppt Cl estimate of Carpenter et al. (2014). However, our BASE run contribution from $COCl_2$ (~5 ppt Cl) is a factor of 3 lower than their "best estimate" of 15 (0–30) ppt Cl, while within the large uncertainty range. In the supporting information, we discuss the uncertainties of our $COCl_2$ simulation (Text S2) and compare modeled $COCl_2$ profiles to ACE data (Figure S6).

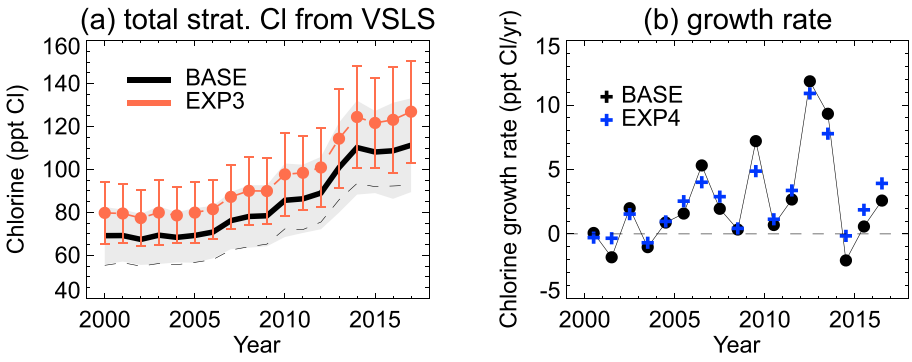

Figure 5. Time series of modeled (a) total stratospheric chlorine input from Cl-VSLS (ppt Cl) and (b) the corresponding growth rate (ppt Cl/year). In panel (a) model output is from the BASE simulation and shows the annual average (black line) total stratospheric chlorine injection (i.e., the sum of source and product gas contributions) with ±1 standard deviation (gray shading). Note, the thin dashed line (black) shows the BASE contribution from source gases only. Also shown is the total stratospheric chlorine injection from EXP3 (orange line, product gas injection upper limit). In panel (b) output from EXP4 (repeating meteorology) is shown in addition to the BASE simulations. VSLS = very short-lived substances.

Although our idealized model setup does not include a detailed, explicit treatment of tropospheric PG chemistry, a simple upper limit estimate for PGI is obtained from EXP3. This experiment assumed no tropospheric removal of $COCl_2$ or Cl_y and is denoted in Figure 4f by the black dashed line. From EXP3, our upper limit of total PGI is ~34.2 (±7.4) ppt Cl in 2017, approximately 80% larger than the BASE run. Both the BASE and EXP3 model estimates are within the large uncertainty range (0–50 ppt Cl) of current assessments (Carpenter et al., 2014). Our analysis constrains the lower end of this range and shows that a nonzero PGI contribution is likely. However, we also note that chlorine PGI due to $COCl_2$ (and hence total PGI) could be underestimated in our model. Both the BASE run and EXP3 underestimate measured $COCl_2$ around the tropical tropopause from the ACE mission by around a factor of 3 (see supporting information). On the one hand, this does not necessarily imply an underestimation of $COCl_2$ produced by Cl-VSLS, given that $COCl_2$ is also a product of long-lived CCl_4 and CH_3CCl_3 degradation (section 2.3). On the other, we note that EXP8, which had a larger assumed fixed yield of $COCl_2$ production from CH_2Cl_2 (see section 2.4), provides much better agreement to the ACE measurements (Figure S6). In summary, factoring in the full range of simulations performed here, modeled chlorine PGI due to VSLS-produced $COCl_2$ is ~5 ppt Cl (BASE run, Table 4) and ~18 ppt Cl (EXP8) in 2017; that is, uncertain by a factor of >3.

4.4. Total Stratospheric Chlorine Injection and Trends

Figure 5 shows the evolution of total stratospheric chlorine ($VSLCl_{tot}$) from VSLS (i.e., the sum of SGI and PGI contributions) over the full simulation period. From the BASE run, we estimate that $VSLCl_{tot}$ increased from ~69 (±14) ppt Cl in 2000, to ~111 (±22) ppt Cl in 2017: that is, a ~61% increase over the 18-year period. Chlorine from CH_2Cl_2 is the largest contributor to $VSLCl_{tot}$ accounting for ~68% of the total, followed by $CHCl_3$ (~19%), $C_2H_4Cl_2$ (~10%), and C_2Cl_4 (~3%). The contribution from C_2HCl_3 is negligible. For individual species, the relative importance of SGI versus PGI varies (Table 4), though SGI dominates $VSLCl_{tot}$ overall, accounting for >80% of the total. This is due to modest relative PGI contributions (<20%) from the principal compounds CH_2Cl_2 and $CHCl_3$, which have the longest tropospheric lifetimes (e.g., Table 1). Our BASE run estimate of $VSLCl_{tot}$ (111 ± 22 ppt Cl in 2017) is slightly larger than the best estimate of 95 (50–145) ppt Cl reported by Carpenter et al. (2014), though within their range of uncertainty. The difference between these estimates reflects the different periods under consideration. Our estimate is an up-to-date assessment based on the most recent observed Cl-VSLS surface trends.

Results from model run EXP3 provide an upper limit to $VSLCl_{tot}$ from our study (see Figure 5a). This experiment does not include tropospheric wet removal of $COCl_2$ or Cl_y PGs and thus assumes their efficient transport to the stratosphere, once produced. From EXP3, $VSLCl_{tot}$ is 126 (±24) ppt Cl in 2017, that is, ~14% larger than the BASE model. The results from this and all other sensitivity experiments are summarized in Figure S7. We find that $VSLCl_{tot}$ is fairly insensitive to changes in tropospheric [OH]; increasing/decreasing [OH] by 25%

(EXP5 and EXP6) leads to only a ~2% decrease/increase in $VSLCl_{tot}$. Comparing EXP4 (repeating 2000 meteorology) to the BASE run (evolving meteorology) shows a relatively small influence of interannual meteorological variability, with $VSLCl_{tot}$ ~1% larger in the former run. While this analysis is not exhaustive, details of tropospheric transport processes will be less important for Cl-VSLS (e.g., CH_2Cl_2 and $CHCl_3$) compared to analogous brominated compounds (e.g., Liang et al., 2014; Tegtmeier et al., 2012), owing to much longer tropospheric lifetimes of the former. Similarly, the importance of Cl atoms as a C_2Cl_4 sink notwithstanding (Figure S7c and section 4.2), the overall influence of Cl atom oxidation of Cl-VSLS on $VSLCl_{tot}$ is small (<0.5%).

Of all parameters examined in the sensitivity experiments, the largest influence on $VSLCl_{tot}$ comes from changing the CH_2Cl_2 surface boundary condition (SG_{MF}) from one derived from NOAA data (BASE run) to one derived from AGAGE (EXP1). In the tropical band 0–30°N, the latter is ~19 ppt lower in 2016 (Figure S1) and its use translates to a ~18% decrease in $VSLCl_{tot}$ overall (EXP1 relative to BASE). These differences between the two networks for CH_2Cl_2 have been previously noted and likely reflect differences in calibration scales (of the order of ~10%) and the different sampling locations (Carpenter et al., 2014). A detailed examination of differences between the measurement networks is beyond the scope of the paper. However, in terms of sampling location within the 0–30°N band, we note that NOAA data are obtained from a Pacific site, while AGAGE data are from an Atlantic one. As noted in section 3, aircraft measurements of CH_2Cl_2 at the point of stratospheric entry (reported on a scale consistent with NOAA) are well reproduced by our BASE model.

Modeled growth rates of $VSLCl_{tot}$, while found to be highly variable (Figure 5b), remained positive year-to-year in the period 2004/2005 to 2013/2014. The start of this period corresponds roughly to the onset of the recently observed increases in CH_2Cl_2 (e.g., Hossaini et al., 2015a). We find that post 2014, $VSLCl_{tot}$ growth rates turned negative for the first time since prior to 2004; for the 2014/2015 period the $VSLCl_{tot}$ growth rate was −2.1 ppt/year Cl in the BASE simulation. In subsequent years, growth was positive at 0.6 ppt Cl/year for 2015/2016 and 2.6 ppt Cl/year for 2016/2017; small in comparison to growth in the 2012/2013 and 2013/2014 periods, for example. The relative slow growth in these most recent years mainly reflects a stabilization in CH_2Cl_2, which is present in the surface boundary conditions forcing the model (Figure S1). This can be seen in the leveling off of the modeled CH_2Cl_2 abundance in the tropical upper troposphere (Figure 3). Continued CH_2Cl_2 observations in coming years will be required to assess whether the above is a transient effect, or rather a longer-term stabilization of CH_2Cl_2 mole fractions/emissions. However, we note that in the context of the full simulation period (Figure 5b), sporadic years of near-zero $VSLCl_{tot}$ growth are somewhat typical, and that the apparent slower growth in the most recent years is also slightly influenced by meteorology (i.e., comparing the blue and black data in Figure 5b).

Although the contribution of VSLS to stratospheric chlorine has increased in absolute terms since the early 2000s, it remains small in comparison to the chlorine provided by long-lived halocarbons (i.e., CFCs, HCFCs, CCl_4, CH_3Cl, etc.). A simple estimate of stratospheric chlorine from long-lived halocarbons is presented in Figure S8. This is based on the surface abundance of the major compounds provided by the WMO A1 scenario (WMO, 2014), and the assumption that 100% of the surface chlorine from these compounds reaches the stratosphere. From the BASE simulation, we estimate that Cl-VSLS accounted for ~2% of stratospheric chlorine in 2000, rising to ~3.4% in 2017. This figure will likely increase further if Cl-VSLS abundances increase in coming years, against a backdrop of declining chlorine from long-lived compounds following the A1 scenario.

4.5. Influence of Chlorinated VSLS on Stratospheric HCl Trends

In the previous section, we discussed the temporal evolution of stratospheric chlorine from VSLS and time-varying growth rates. An ordinary least squares fit to the full time series of data in Figure 5a (2000–2017) suggests total chlorine from VSLS ($VSLCl_{tot}$) increased at a mean rate of ~2.9 (±0.3) ppt Cl/year. Over the shorter 2004–2017 period, roughly corresponding to the onset of significant CH_2Cl_2 growth in the mid-2000s, the trend is 3.8 (±0.3) ppt Cl/year—in good agreement with our earlier estimates (Hossaini et al., 2015b). Note that changes to CH_2Cl_2 dominate the trend in $VSLCl_{tot}$. For example, without CH_2Cl_2 included, the 2004–2017 trend is reduced to ~0.23 (±0.06) ppt Cl/year, reflecting small increases in $CHCl_3$ over the period (e.g., Figure 3b).

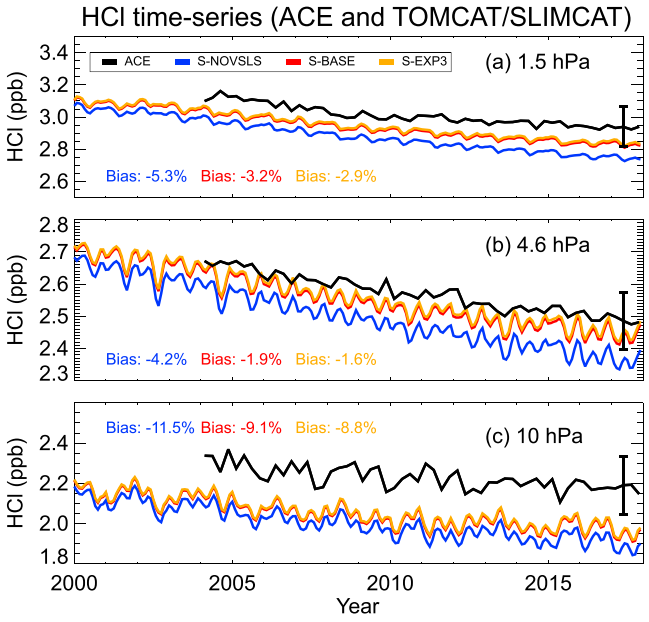

Figure 6. Modeled versus observed HCl (ppb) at (a) 1.5, (b) 4.6, and (c) 10 hPa between 60°N and 60°S latitude. The observed satellite data are from the ACE instrument (section 3.2). Annotated biases (model − observation, %) are shown for experiments S-BASE (red), S-EXP3 (orange), and S-NOVSLS (blue). The vertical error bar (shown illustratively for 2017) represents the 1σ ACE HCl measurement error, ~0.12 ppb.

To provide additional "top down" constraints on the magnitude of historical trends in stratospheric chlorine from VSLS, we consider satellite observations (section 3.2) of stratospheric HCl (2004–2017) from the ACE satellite mission (Bernath & Fernando, 2018). Our analysis focusses on the upper stratosphere (pressures less than ~10 hPa) where HCl is far less affected by dynamical variability relative to the lower stratosphere (e.g., Stolarski et al., 2018). Four additional integrations of the stratospheric configuration of TOMCAT/SLIMCAT were performed. The first stratospheric simulation (referred to as "S-NOVSLS") contained no chlorine from VSLS. The second (S-BASE) considered time-dependent stratospheric loadings of $CHCl_3$, CH_2Cl_2, C_2Cl_4, and $C_2H_4Cl_2$ (Figure 3) and their associated PGs (Figure 4), based on values from the BASE simulation. As the dynamics are the same in both runs, the impact of VSLS growth on HCl trends can be isolated readily. The third stratospheric simulation (S-EXP3) was identical to the above but stratospheric VSLS loadings were taken from EXP3 (i.e., PGI upper limit). Finally, S-FIXDYN was identical to S-BASE but employed repeating year-2000 dynamics. This allowed us to examine the relative influence of chemistry versus dynamics on simulated HCl trends. All simulations were performed for the period 2000 to 2017. The version of the stratospheric model employed here was recently used by Chipperfield et al. (2018) to investigate lower stratospheric ozone trends and is used by Harrison et al. (2018) to interpret long-term $COCl_2$ observations from ACE. It has also been extensively evaluated in terms of both chemistry and transport (e.g., Harrison et al., 2016; Wales et al., 2018).

Figure 6 compares the modeled upper stratospheric HCl time series (60°S–60°N) to that observed by ACE. The model-measurement agreement is generally very good, with biases (see annotations on figure) ~12% or less. Model runs with additional chlorine from VSLS included (runs S-BASE and S-EXP3) exhibit a lower model-measurement bias (relative to run S-NOVSLS) by several percent. However, we also note the size of the ACE measurement error is comparable to $VSLCl_{tot}$ in 2017 (around ±0.12 ppb). Bernath and Fernando (2018) provided an up-to-date assessment of stratospheric HCl trends based on these ACE data. Between 60°S and 60°N, they estimated a mean rate of HCl decline of −4.8 (±0.7)% per decade in the upper stratosphere (pressures less than 1.5 hPa, ~45–51 km) between 2004 and 2017. In the upper stratosphere, HCl is most abundant, provides a proxy for total atmospheric chlorine, and is where the trend is least uncertain. The vertically resolved ACE HCl trends for different latitudes and equivalent model estimates are given in Figure 7. Note, in order to perform a like-for-like comparison to the model, the ACE trend data here does not incorporate N_2O into the trend analysis (Bernath & Fernando, 2018).

Figure 7 highlights the major influence of dynamical variations (i.e., comparing S-FIXDYN and S-BASE) in the lower stratosphere and a contrasting dynamical influence in the two midlatitude regions (Figure 7c vs 7d). In the midlatitude lower stratosphere, the sign and magnitude of the model trends (e.g., S-BASE) agree reasonably well to those from ACE considering the large uncertainty. Away from the lower stratosphere (at higher altitude), HCl trends are far less sensitive to dynamical variability (e.g., Stolarski et al., 2018), which is apparent from the model data in Figure 7 (i.e., the convergence of the red and dashed green lines above 10 hPa).

In the upper stratosphere (pressure ≤10 hPa), the modeled and observed trends are in reasonable agreement. Note, at pressures less than ~5 hPa, the 2σ error bars do not overlap for the with/without VSLS trend estimates from the model. Between 60°S and 60°N, the mean HCl trend in the upper stratosphere is −5.0 (±0.3)% per decade from S-FIXDYN, in close agreement (~4% larger) to the ACE trend of −4.8 (±0.7)% per decade (Table S3). HCl trends from S-BASE (−5.2 ± 0.3% per decade) and S-NOVSLS (−6.1 ± 0.2% per decade) are ~8% and ~27% larger the ACE value, respectively. The difference between these two model runs reveals a 15% slower rate of upper stratospheric HCl decline, attributable solely to the inclusion of Cl-

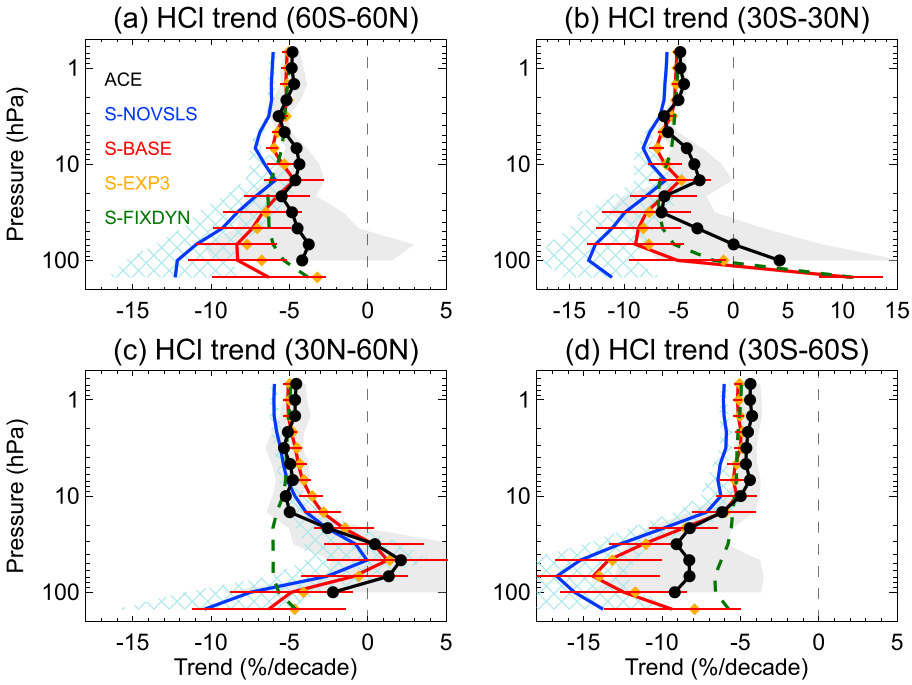

Figure 7. Comparison of stratospheric HCl trends (% per decade) from ACE satellite observations (Bernath & Fernando, 2018) and model runs (2004–2017). Mean trends are for (a) 60°S to 60°N, (b) 30°S to 30°N, (c) 30 to 60°N, and (d) 30 to 60°S. Horizontal error bars on model run S-BASE denote 2σ errors, also represented by hatching and gray shading.

VSLS. The S-NOVSLS trend is in close agreement to the observed rate of change in total tropospheric chlorine measured by NOAA (−6.1 ± 0.09% per decade for 2004–2016) when excluding Cl-VSLS, and with a 7-year time lag applied to the NOAA time series (Figure S9) to account for transport time to the upper stratosphere. The HCl trend from S-EXP3, with a greater loading of chlorine from Cl-VSLS relative to S-BASE, is also shown in Figure 7. In the upper stratosphere, the S-EXP3 trend (−5.1 ± 0.3% per decade) is similar to the BASE run.

Overall, the above comparisons show that the model provides a reasonable representation of observed stratospheric HCl trends, including when Cl-VSLS are considered. While we acknowledge that HCl trends from models and measurements are uncertain, the upper stratospheric trend analysis provides further evidence that VSLS may have offset some of the possible benefits of the Montreal Protocol in reducing stratospheric chlorine over the last decade. Our simulations indicate that upper stratospheric HCl has declined at a 15% slower rate globally over the 2004–2017 period due to VSLS, relative to what would be expected in their absence.

5. Summary and Concluding Remarks

We have performed 3-D CTM simulations and analyzed observation data to (a) quantify the stratospheric input of chlorine from VSLS (CH_2Cl_2, $CHCl_3$, C_2Cl_4, $C_2H_4Cl_2$, and C_2HCl_3) between 2000 and 2017, (b) quantify its sensitivity to a range of factors (including assumptions in model chemistry and model transport), and (c) examine if inclusion of Cl-VSLS improves the model representation of stratospheric HCl trends. Our main findings and recommendations for future research are summarized below:

1. Stratospheric chlorine SGI from VSLS increased from ~55 (±10) ppt Cl in 2000 to ~93 (±17) ppt Cl in 2017. CH_2Cl_2 accounts for ~70% of the present-day total. Observations from NASA campaigns (2004–2016) show increasing CH_2Cl_2 around the tropical tropopause, consistent in magnitude to modeled increases and corroborating reported increases from independent surface (Hossaini et al., 2015a; Hossaini et al., 2017) and upper tropospheric (Leedham Elvidge et al., 2015) records. Total chlorine SGI observed during the 2015 VIRGAS (104 ± 15 ppt Cl) and 2016 POSIDON missions (120 ± 27 ppt Cl) agree well with our model (to within a few percent, when the model is sampled during the

campaign periods). Total SGI is insensitive to inclusion of tropospheric Cl atom oxidation of VSLS in our model (when [Cl] = 1.3×10^3 atoms per cubic centimeter). However, the C_2Cl_4 + Cl reaction is significant, with its inclusion (a) reducing the C_2Cl_4 lifetime by up to ~50% at 10 km and (b) greatly improving C_2Cl_4 model-measurement agreement around the tropopause.

2. As is the case with brominated VSLS, estimation of stratospheric PGI is challenging owing to the complexity of the chemical processes involved. Our simulations considered total PGI from $COCl_2$ (produced by $CHCl_3$, CH_2Cl_2, and C_2Cl_4) and from an idealized Cl_y tracer (produced by all), both of which had prescribed tropospheric lifetimes based on the literature. We estimate a nonzero chlorine PGI from VSLS of ~18 (±5) ppt Cl in 2017, within the 0–50 ppt Cl range reported in WMO (2014). When assuming no tropospheric wet removal of $COCl_2$ and Cl_y, this estimate increases to ~34 (±7) ppt Cl. Our parameterized scheme suggests $COCl_2$ is a product of CH_2Cl_2 degradation, particularly in low NO_x regions. However, modeled $COCl_2$ near the tropical tropopause is underestimated by a factor of ~3 and further work to elucidate the uncertain mechanism of $COCl_2$ production is needed.
3. Total stratospheric Cl from VSLS ($VSLCl_{tot}$) increased by ~61% between 2000 (~69 ± 14 ppt Cl) and 2017 (~111 ± 22 ppt Cl). In the same years, VSLS represented ~2% and ~3.4% of overall stratospheric chlorine —a small but significant portion that should increase given the ongoing decline of long-lived chlorine (e.g., CFCs) under the Montreal Protocol. A sensitivity experiment in which PGs from VSLS were not removed in the troposphere by deposition processes gives a 2017 $VSLCl_{tot}$ upper limit of 126 (±24) ppt Cl. We estimate $VSLCl_{tot}$ increased by 3.8 (±0.3) ppt Cl/year between 2004 and 2017, with CH_2Cl_2 changes dominating the trend. Growth was negative or slow in the period 2014/2015 to 2016/2017, relative to much larger growth in 2012/2013 and 2013/2014. Further observations to determine whether this is a transient effect are needed.
4. Increasing stratospheric chlorine from VSLS between 2004 and 2017 will have likely had a small but significant influence on HCl trends in the upper stratosphere. Measurements from the ACE satellite mission show a mean rate of upper stratospheric HCl decline of −4.8% per decade between 2004 and 2017, compared to model trends of −5.1 to −5.2% per decade with VSLS, and −6.1% per decade without.

In conclusion, the contribution of VSLS to total stratospheric chlorine remains small in both absolute and relative terms. However, our results provide evidence that VSLS have acted to offset the rate of chlorine decline in the stratosphere, and therefore some of the possible benefits of the Montreal Protocol since the mid-2000s. Given suggestions that anthropogenic CH_2Cl_2 emissions from major economies will increase in the coming decade (Feng et al., 2018), such an offset may continue.

Acknowledgments
This work was supported by RH's NERC Independent Research Fellowship (NE/N014375/1) and the NERC SISLAC project (NE/R001782/1). J.J.H. wishes to thank UKRI - NERC for funding via the National Centre for Earth Observation, contract PR140015. The ACE mission is funded primarily by the Canadian Space Agency. ACE-FTS data can be obtained from https://databace.scisat.ca/level2/ace_v3.5_v3.6/. AGAGE operations at Mace Head, Trinidad Head, Cape Matatula, Ragged Point, and Cape Grim are supported by the National Aeronautics and Space Administration (NASA) with grants NAG5-12669, NNX07AE89G, NNX11AF17G, and NNX16AC98G to MIT, grants NNX07AE87G, NNX07AF09G, NNX11AF15G, and NNX11AF16G to SIO; by the Department for Business, Energy & Industrial Strategy (BEIS) contract 1028/06/2015 to the University of Bristol for Mace Head; by the National Oceanic and Atmospheric Administration (NOAA, USA) contract RA-133-R15-CN-0008 to the University of Bristol for Barbados; by the Commonwealth Scientific and Industrial Research Organization (CSIRO Australia), and the Bureau of Meteorology (Australia) for Cape Grim. The model simulations were performed on the national Archer and Leeds ARC HPC facilities. NOAA data used to calculate model boundary conditions is available at https://www.esrl.noaa.gov/gmd/. The AGAGE data are available at https://agage.mit.edu/data/agage-data. The model data itself will be uploaded to the Lancaster University data repository on acceptance of the article. The supporting information to this article consists of nine figures and three tables.

References

Atkinson, R., Baulch, D. L., Cox, R. A., Crowley, J. N., Hampson, R. F., Hynes, R. G., et al. (2008). Evaluated kinetic and photochemical data for atmospheric chemistry: Volume IV—Gas phase reactions of organic halogen species. *Atmospheric Chemistry and Physics*, *8*, 4141–4496. https://doi.org/10.5194/acp-8-4141-2008

Bernath, P., & Fernando, A. M. (2018). Trends in stratospheric HCl from the ACE satellite mission. *Journal of Quantitative Spectroscopy & Radiative Transfer*, *217*, 126–129. https://doi.org/10.1016/j.jqsrt.2018.05.027

Bernath, P. F. (2017). The atmospheric chemistry experiment (ACE). *Journal of Quantitative Spectroscopy & Radiative Transfer*, *186*, 3–16. https://doi.org/10.1016/j.jqsrt.2016.04.006

Brown, A. T., Chipperfield, M. P., Boone, C., Wilson, C., Walker, K. A., & Bernath, P. F. (2011). Trends in atmospheric halogen containing gases since 2004. *Journal of Quantitative Spectroscopy & Radiative Transfer*, *112*(16), 2552–2566. https://doi.org/10.1016/j.jqsrt.2011.07.005

Burkholder, J. B., Sander, S. P., Abbatt, J. P. D., Barker, J. R., Huie, R. E., Kolb, C. E., et al. (2015). *Chemical kinetics and photochemical data for use in atmospheric studies, Evaluation Nnumber 18, JPL Publication 15–10*. Pasadena, CA: Jet Propulsion Laboratory.

Carpenter, L. J., Reimann, S., Burkholder, J. B., Clerbaux, C., Hall, B., Hossaini, R., et al. (2014). Ozone-depleting substances (ODSs) and other gases of interest to the Montreal Protocol. In *Scientific Assessment of Ozone Depletion: 2014, in Global Ozone Research and Monitoring Project, Report No. 55* (Chap. 1). Geneva, Switzerland: World Meteorol. Organ.

Catoire, V., Lesclaux, R., Schneider, W. F., & Wallington, T. J. (1996). Kinetics and mechanisms of the self-reactions of CCl_3O_2 and $CHCl_2O_2$ radicals and their reactions with HO_2. *The Journal of Physical Chemistry*, *100*(34), 14,356–14,371. https://doi.org/10.1021/jp960572z

Chipperfield, M. P. (2006). New version of the TOMCAT/SLIMCAT off-line chemical transport model: Intercomparison of stratospheric tracer experiments. *Quarterly Journal of the Royal Meteorological Society*, *132*(617), 1179–1203. https://doi.org/10.1256/qj.05.51

Chipperfield, M. P., Bekki, S., Dhomse, S., Harris, N. R. P., Hassler, B., Hossaini, R., et al. (2017). Detecting recovery of the stratospheric ozone layer. *Nature*, *549*, 211–218. https://doi.org/10.1038/nature23681

Chipperfield, M. P., Dhomse, S., Hossaini, R., Feng, W., Santee, M. L., Weber, M., et al. (2018). On the cause of recent variations in lower stratospheric ozone. *Geophysical Research Letters*, *45*, 5718–5726. https://doi.org/10.1029/2018GL078071

Christiansen, C. J., & Francisco, J. S. (2010a). Atmospheric oxidation of tetrachloroethylene: An ab initio study. *The Journal of Physical Chemistry. A*, *114*(34), 9177–9191. https://doi.org/10.1021/jp103845h

Christiansen, C. J., & Francisco, J. S. (2010b). Atmospheric oxidation of trichloroethylene: An ab initio study. *The Journal of Physical Chemistry. A*, *114*(34), 9163–9176. https://doi.org/10.1021/jp103769z

Dee, D. P., Uppala, S. M., Simmons, A. J., Berrisford, P., Poli, P., Kobayashi, S., et al. (2011). The ERA-Interim reanalysis: Configuration and performance of the data assimilation system. *Quarterly Journal of the Royal Meteorological Society*, *137*(656), 553–597. https://doi.org/10.1002/qj.828

Dhomse, S. S., Chipperfield, M. P., Damadeo, R. P., Zawodny, J. M., Ball, W. T., Feng, W., et al. (2016). On the ambiguous nature of the 11 year solar cycle signal in upper stratospheric ozone. *Geophysical Research Letters*, *43*, 7241–7249. https://doi.org/10.1002/2016GL069958

Dhomse, S. S., Kinnison, D., Chipperfield, M. P., Salawitch, R. J., Cionni, I., Hegglin, M. I., et al. (2018). Estimates of ozone return dates from chemistry-climate model initiative simulations. *Atmospheric Chemistry and Physics*, *18*, 8409–8438. https://doi.org/10.5194/acp-18-8409-2018

Dhomse, S. S., Chipperfield, M. P., Feng, W., Hossaini, R., Mann, G. W., & Santee, M. L. (2015). Revisiting the hemispheric asymmetry in mid-latitude ozone changes following the Mount Pinatubo eruption: A 3-D model study. *Geophysical Research Letters*, *42*, 3038–3047. https://doi.org/10.1002/2015GL063052

Eyring, V., Cionni, I., Bodeker, G. E., Charlton-Perez, A. J., Kinnison, D. E., Scinocca, J. F., et al. (2010). Multi-model assessment of stratospheric ozone return dates and ozone recovery in CCMVal-2 models. *Atmospheric Chemistry and Physics*, *10*, 9451–9472. https://doi.org/10.5194/acp-10-9451-2010

Feng, W., Chipperfield, M. P., Dhomse, S., Monge-Sanz, B. M., Yang, X., Zhang, K., & Ramonet, M. (2011). Evaluation of cloud convection and tracer transport in a three-dimensional chemical transport model. *Atmospheric Chemistry and Physics*, *11*(12), 5783–5803. https://doi.org/10.5194/acp-11-5783-2011

Feng, Y., Bie, P., Wang, Z., Wang, L., & Zhang, J. (2018). Bottom-up anthropogenic dichloromethane emission estimates from China for the period 2005–2016 and predictions of future emissions. *Atmospheric Environment*, *186*, 241–247. https://doi.org/10.1016/j.atmosenv.2018.05.039

Froidevaux, L., Livesey, N. J., Read, W. G., Salawitch, R. J., Waters, J. W., Drouin, B., et al. (2006). Temporal decrease in upper atmospheric chlorine. *Geophysical Research Letters*, *33*, L23812. https://doi.org/10.1029/2006GL027600

Fu, D., Boone, C. D., Bernath, P. F., Walker, K. A., Nassar, R., Manney, G. L., & McLeod, S. D. (2007). Global phosgene observations from the atmospheric chemistry experiment (ACE) mission. *Geophysical Research Letters*, *34*, L17815. https://doi.org/10.1029/2007GL029942

Hagan, D. E., Webster, C. R., Farmer, C. B., May, R. D., Herman, R. L., Weinstock, E. M., et al. (2004). Validating AIRS upper atmosphere water vapor retrievals using aircraft and balloon in situ measurements. *Geophysical Research Letters*, *31*, L21103. https://doi.org/10.1029/2004GL020302

Harrison, J. J., Chipperfield, M. P., Boone, C. D., Dhomse, S. S., Bernath, P. F., Froidevaux, L., et al. (2016). Satellite observations of stratospheric hydrogen fluoride and comparisons with SLIMCAT calculations. *Atmospheric Chemistry and Physics*, *16*, 10,501–10,519. https://doi.org/10.5194/acp-16-710501-2016

Harrison, J. J., Chipperfield, M. P., Hossaini, R., Boone, C. D., Dhomse, S., Feng, W., & Bernath, P. F. (2018). Phosgene in the upper troposphere and lower stratosphere: A marker for product gas injection due to chlorine-containing very short-lived substances. *Geophysical Research Letters*, *45*. https://doi.org/10.1029/2018GL079784

Holtslag, A., & Boville, B. (1993). Local versus nonlocal boundary-layer diffusion in a global climate model. *Journal of Climate*, *6*(10), 1825–1842. https://doi.org/10.1175/1520-0442(1993)006<1825:LVNBLD>2.0.CO;2

Hossaini, R., Chipperfield, M. P., Monge-Sanz, B. M., Richards, N. A. D., Atlas, E., & Blake, D. R. (2010). Bromoform and dibromomethane in the tropics: A 3-D model study of chemistry and transport. *Atmospheric Chemistry and Physics*, *10*, 719–735. https://doi.org/10.5194/acp-10-719-2010

Hossaini, R., Chipperfield, M. P., Montzka, S. A., Leeson, A. A., Dhomse, S., & Pyle, J. A. (2017). The increasing threat to stratospheric ozone from dichloromethane. *Nature Communications*, *8*, 15962. https://doi.org/10.1038/ncomms15962

Hossaini, R., Chipperfield, M. P., Montzka, S. A., Rap, A., Dhomse, S., & Feng, W. (2015a). Efficiency of short-lived halogens at influencing climate through depletion of stratospheric ozone. *Nature Geoscience*, *8*, 186–190. https://doi.org/10.1038/ngeo2363

Hossaini, R., Chipperfield, M. P., Saiz-Lopez, A., Harrison, J. J., von Glasow, R., Sommariva, R., et al. (2015b). Growth in stratospheric chlorine from short-lived chemicals not controlled by the Montreal Protocol. *Geophysical Research Letters*, *42*, 4573–4580. https://doi.org/10.1002/2015GL063783

Hossaini, R., Chipperfield, M. P., Saiz-Lopez, A., Fernandez, R., Monks, S., Feng, W., et al. (2016a). A global model of tropospheric chlorine chemistry: Organic versus inorganic sources and impact on methane oxidation. *Journal of Geophysical Research: Atmospheres*, *121*, 14,271–14,297. https://doi.org/10.1002/2016JD025756

Hossaini, R., Patra, P. K., Leeson, A. A., Krysztofiak, G., Abraham, N. L., Andrews, S. J., et al. (2016b). A multi-model intercomparison of halogenated very short-lived substances (TransCom-VSLS): Linking oceanic emissions and tropospheric transport for a reconciled estimate of the stratospheric source gas injection of bromine. *Atmospheric Chemistry and Physics*, *16*, 9163–9187. https://doi.org/10.5194/acp-16-9163-2016

Jensen, E. J., Pfister, L., Jordan, D. E., Bui, T. V., Ueyama, R., Singh, H. B., et al. (2017). The NASA airborne tropical tropopause experiment: High-altitude aircraft measurements in the tropical Western Pacific. *Bulletin of the American Meteorological Society*, *98*, 129–143. https://doi.org/10.1175/BAMS-D-14-00263.1

Kindler, T. P., Chameides, W. L., Wine, P. H., Cunnold, D. M., Alyea, F. N., & Franklin, J. A. (1995). The fate of atmospheric phosgene and the stratospheric chlorine loadings of its parent compounds: CCl_4, C_2Cl_4, C_2HCl_3, CH_3CCl_3, and $CHCl_3$. *Journal of Geophysical Research*, *100*, 1235–1251. https://doi.org/10.1029/94JD02518

Ko, M. K. W., Poulet, G., Blake, D. R., Boucher, O., Burkholder, J. H., Chin, M., et al. (2003). Halogenated very short-lived substances. In *Scientific Assessment of Ozone Depletion: 2006, in Global Ozone Research and Monitoring Project, Report No. 50* (Chap. 2). Geneva, Switzerland: World Meteorological Organization.

Leedham Elvidge, E. C., Oram, D. E., Laube, J. C., Baker, A. K., Montzka, S. A., Humphrey, S., et al. (2015). Increasing concentrations of dichloromethane, CH_2Cl_2, inferred from CARIBIC air samples collected 1998–2012. *Atmospheric Chemistry and Physics*, *15*, 1939–1958. https://doi.org/10.5194/acp-15-1939-2015

Liang, Q., Atlas, E., Blake, D., Dorf, M., Pfeilsticker, K., & Schauffler, S. (2014). Convective transport of very short lived bromocarbons to the stratosphere. *Atmospheric Chemistry and Physics*, *14*, 5781–5792. https://doi.org/10.5194/acp-14-5781-2014

McNorton, J., Chipperfield, M. P., Gloor, M., Wilson, C., Feng, W., Hayman, G. D., et al. (2016). Role of OH variability in the stalling of the global atmospheric CH4 growth rate from 1999 to 2006. *Atmospheric Chemistry and Physics*, *16*, 7943–7956. https://doi.org/10.5194/acp-16-7943-2016

Monks, S. A., Arnold, S. R., Hollaway, M. J., Pope, R. J., Wilson, C., Feng, W., et al. (2017). The TOMCAT global chemical transport model v1.6: Description of chemical mechanism and model evaluation. *Geoscientific Model Development*, *10*, 3025–3057. https://doi.org/10.5194/gmd-10-3025-2017

Montzka, S. A., Butler, J. H., Hall, B. D., Mondeel, D. J., & Elkins, J. W. (2003). A decline in tropospheric organic bromine. *Geophysical Research Letters*, *30*(15), 1826. https://doi.org/10.1029/2003GL017745

Montzka, S. A., Dutton, G. S., Yu, P., Ray, E., Portmann, R. W., Daniel, J. S., et al. (2018). An unexpected and persistent increase in global emissions of ozone-depleting CFC-11. *Nature*, *557*, 413–417. https://doi.org/10.1038/s41586-018-0106-2

Montzka, S. A., Reimann, S., Engel, A., Krüger, K., O'Doherty, S., Sturges, W. T., et al. (2011). Ozone-depleting substances (ODSs) and related chemicals. In *Scientific assessment of ozone depletion: 2010*, *Global Ozone Res. and Monit. Proj.-Rep. 52* (Chap. 1, pp. 1–112). Geneva, Switzerland: World Meteorol. Organ.

Navarro, M. A., Atlas, E. L., Saiz-Lopez, A., Rodriguez-Lloveras, X., Kinnison, D. E., Lamarque, J., et al. (2015). Airborne measurements of organic bromine compounds in the Pacific tropical tropopause layer. *Proceedings of the National Academy of Sciences of the United States of America*, *112*(45), 13,789–13,793. https://doi.org/10.1073/pnas.1511463112

Oram, D. E., Ashfold, M. J., Laube, J. C., Gooch, L. J., Humphrey, S., Sturges, W. T., et al. (2017). A growing threat to the ozone layer from short-lived anthropogenic chlorocarbons. *Atmospheric Chemistry and Physics*, *17*, 11,929–11,941. https://doi.org/10.5194/acp-17-11929-2017

Park, S., Jiménez, R., Daube, B. C., Pfister, L., Conway, T. J., Gottlieb, E. W., et al. (2007). The CO_2 tracer clock for the tropical tropopause layer. *Atmospheric Chemistry and Physics*, *7*, 3989–4000. https://doi.org/10.5194/acp-7-3989-2007

Patra, P. K., Houweling, S., Krol, M., Bousquet, P., Belikov, D., Bergmann, D., et al. (2011). TransCom model simulations of CH4 and related species: Linking transport, surface flux and chemical loss with CH4 variability in the troposphere and lower stratosphere. *Atmospheric Chemistry and Physics*, *11*(24), 12,813–12,837. https://doi.org/10.5194/acp-11-12813-2011

Pfister, L., Selkirk, H. B., Starr, D. O., Rosenlof, K., & Newman, P. A. (2010). A meteorological overview of the TC4 mission. *Journal of Geophysical Research*, *115*, D00J12. https://doi.org/10.1029/2009JD013316

Prather, M. (1986). Numerical advection by conservation of 2nd-order moments. *Journal of Geophysical Research*, *91*, 6671–6681. https://doi.org/10.1029/JD091iD06p06671

Prinn, R. G., Weiss, R. F., Fraser, P. J., Simmonds, P. G., Cunnold, D. M., Alyea, F. N., et al. (2000). A history of chemically and radiatively important gases in air deduced from ALE/GAGE/AGAGE. *Journal of Geophysical Research*, *105*(D14), 17,751–17,792. https://doi.org/10.1029/2000JD900141

Richards, N. A. D., Arnold, S. R., Chipperfield, M. P., Miles, G., Rap, A., Siddans, R., et al. (2013). The Mediterranean summertime ozone maximum: global emission sensitivities and radiative impacts. *Atmospheric Chemistry and Physics*, *13*, 2331–2345. https://doi.org/10.5194/acp-13-2331-2013

Sala, S., Bönisch, H., Keber, T., Oram, D. E., Mills, G., & Engel, A. (2014). Deriving an atmospheric budget of total organic bromine using airborne in situ measurements from the western Pacific area during SHIVA. *Atmospheric Chemistry and Physics*, *14*, 6903–6923. https://doi.org/10.5194/acp-14-6903-2014

Salawitch, R. J., Weisenstein, D. K., Kovalenko, L. J., Sioris, C. E., Wennberg, P. O., Chance, K., et al. (2005). Sensitivity of ozone to bromine in the lower stratosphere. *Geophysical Research Letters*, *32*, L05811. https://doi.org/10.1029/2004GL021504

Sanhueza, S., & Heicklen, J. (1975). Chlorine-atom sensitized oxidation of dichloromethane and chloromethane. *The Journal of Physical Chemistry*, *79*(1), 7–11. https://doi.org/10.1021/j100568a002

Sherwen, T., Schmidt, J. A., Evans, M. J., Carpenter, L. J., Großmann, K., Eastham, S. D., et al. (2016). Global impacts of tropospheric halogens (Cl, Br, I) on oxidants and composition in GEOS-Chem. *Atmospheric Chemistry and Physics*, *16*, 12,239–12,271. https://doi.org/10.5194/acp-16-12239-2016

Solomon, S. (1999). Stratospheric ozone depletion: A review of concepts and history. *Reviews of Geophysics*, *37*(3), 275–316. https://doi.org/10.1029/1999RG900008

Solomon, S., Ivy, D. J., Kinnison, D., Mills, M. J., Neely, R. R., & Schmidt, A. (2016). Emergence of healing in the Antarctic ozone layer. *Science*, *353*, 269–274. https://doi.org/10.1126/science.aae0061

Spence, J. W. P., Hanst, L., & Gay, B. W. Jr. (1976). Atmospheric oxidation of methyl chloride, methylene chloride, and chloroform. *Journal of the Air Pollution Control Association*, *26*, 994–996. https://doi.org/10.1080/00022470.1976.10470354

Stolarski, R. S., Douglass, A. R., & Strahan, E. E. (2018). Using satellite measurements of N_2O to remove dynamical variability from HCl measurements. *Atmospheric Chemistry and Physics*, *18*, 5691–5697. https://doi.org/10.5194/acp-18-5691-2018

Sturges, W. T., Oram, D. E., Carpenter, L. J., Penkett, S. A., & Engel, A. (2000). Bromoform as a source of stratospheric bromine. *Geophysical Research Letters*, *27*(14), 2081–2084. https://doi.org/10.1029/2000GL011444

Tegtmeier, S., Krüger, K., Quack, B., Atlas, E. L., Pisso, I., Stohl, A., & Yang, X. (2012). Emission and transport of bromocarbons: From the West Pacific Ocean into the stratosphere. *Atmospheric Chemistry and Physics*, *12*, 10,633–10,648. https://doi.org/10.5194/acp-12-10633-2012

Tiedtke, M. (1989). A comprehensive mass flux scheme for cumulus parameterization in large-scale models. *Monthly Weather Review*, *117*(8), 1779–1800. https://doi.org/10.1175/1520-0493

Toyota, K., Kanaya, Y., Takahashi, M., & Akimoto, H. (2004). A box model study on photochemical interactions between VOCs and reactive halogen species in the marine boundary layer. *Atmospheric Chemistry and Physics*, *4*, 1961–1987. https://doi.org/10.5194/acp-4-1961-2004

Tuazon, E. C., Atkinson, R., Aschmann, S. M., Goodman, M. A., & Winer, A. M. (1988). Atmospheric reactions of chloroethenes with the OH radical. *International Journal of Chemical Kinetics*, *20*, 241–265. https://doi.org/10.1002/kin.550200305

Voulgarakis, A., Naik, V., Lamarque, J. F., Shindell, D. T., Young, P. J., Prather, M. J., et al. (2013). Analysis of present day and future OH and methane lifetime in the ACCMIP simulations. *Atmospheric Chemistry and Physics*, *13*, 2563–2587. https://doi.org/10.5194/acp-13-2563-2013

Wales, P. A., Salawitch, R. J., Nicely, J. M., Anderson, D. C., Canty, T. P., Baidar, S., et al. (2018). Stratospheric injection of brominated very short-lived substances: Aircraft observations in the Western Pacific and representation in global models. *Journal of Geophysical Research: Atmospheres*, *123*, 5690–5719. https://doi.org/10.1029/2017JD027978

Weatherhead, E. C., Reinsel, G. C., Tiao, G. C., Meng, X. L., Choi, D., Cheang, W. K., et al. (1998). Factors affecting the detection of trends: Statistical considerations and applications to environmental data. *Journal of Geophysical Research*, *103*(D14), 17,149–17,161. https://doi.org/10.1029/98JD00995

WMO (2014). Scientific assessment of ozone depletion: 2014 global ozone research and monitoring project report. Geneva, Switzerland: World Meteorological Organization.

Wofsy, S. C., Daube, B. C., Jimenez, R., Kort, E., Pittman, J. V., Park, S., et al. (2012). HIPPO Combined Discrete Flask and GC Sample GHG, Halo-, Hydrocarbon Data (R_20121129). Carbon Dioxide Information Analysis Center, Oak Ridge National Laboratory, Oak Ridge, TN. https://doi.org/10.3334/CDIAC/hippo_012 (Release 20121129).

Wofsy, S. C., the HIPPO Science Team and Cooperating Modellers, & Satellite Teams (2011). HIAPER pole-to-pole observations (HIPPO): Fine-grained, global-scale measurements of climatically important atmospheric gases and aerosols. *Philosophical Transactions of the Royal Society A*, *369*(1943), 2073–2086. https://doi.org/10.1098/rsta.2010.0313